PHYSICAL REVIEW A VOLUME 25, NUMBER 2 FEBRUARY 1982

Electron-impact ionization of Zn^+ and Ga^+

Wade T. Rogers,* G. Stefani,† R. Camilloni,† and Gordon H. Dunn‡
Joint Institute for Laboratory Astrophysics, University of Colorado and National Bureau of Standards, Boulder, Colorado 80309

Alfred Z. Msezane§ and Ronald J. W. Henry
Department of Physics and Astronomy, Louisiana State University, Baton Rouge, Louisiana 70803
(Received 18 May 1981)

Absolute cross sections for electron-impact ionization of Zn^+ and Ga^+ have been measured from below threshold to 2 keV with the use of the crossed-charged-beams technique. Excitation autoionization was shown to be of major importance in both ions for the region between 1 and 2 times threshold, leading to enhancement of the cross sections by factors of up to ~ 2.5. Discrepancies between experiment and the well-known semiempirical formula of Lotz were up to 70%, but reduction of Lotz's a_{3d} coefficient by a factor of 2 leads to satisfactory agreement at high energies. Comparison is also made with scaled-Born-approximation calculations.

I. INTRODUCTION

Electron-impact ionization of positive ions is a major factor in determining the ionization balance in hot, dense plasmas such as those found in stellar atmospheres and fusion-related laboratory plasmas. Owing to recent efforts toward obtaining controlled thermonuclear plasmas as energy sources, the need for accurate experimental data has intensified, and the present work is directed toward this end.

Consider the following ionization mechanisms:

$$X^{+n}+e\rightarrow X^{+(n+1)}+2e\ , \tag{1}$$

$$X^{+n}+e\rightarrow X^{+(n+1)*}+2e \searrow X^{+(n+k)}+(k+1)e\ , \tag{2}$$

$$X^{+n}+e\rightarrow X^{+n*}+e \searrow X^{+(n+k)}+(k+1)e\ . \tag{3}$$

Process (1) represents direct knock-on ionization, while Eqs. (2) and (3) include indirect processes such as inner-shell ionization followed by Auger emission of additional electrons, and excitation autoionization. Not shown in Eqs. (2) or (3) are the many possible stabilization pathways, including radiative processes. It becomes clear that the theoretical obstacles in the treatment of electron-impact ionization are large due to the multiplicity and complexity of possible ionization mechanisms. An additional theoretical difficulty lies in the many-body nature of the problem. Despite these difficulties, theoretical progress has been made in this area. A number of calculations for light ions have been carried out in the Coulomb-Born (CB) approximation,[1–4] and a recent series of systematic theoretical studies have been performed[5] using the distorted wave Born-exchange approximation with comparison to other methods. Sampson and Golden[6] give formulas for computing ionization cross sections for highly charged ions based on scaling of Coulomb-Born calculations for infinitely charged hydrogenic ions in various states. The plane-wave Born (PWB) approximation has been widely compared with data for ionization of ions, largely in attempts to deduce scaling laws.[7–9] These calculations have been carried out for configurations[7] up to $4d^{10}5s^2 5p$. Where CB and PWB calculations have been compared for the same configuration, the near-threshold CB results are consistently higher than the PWBA results due to the focusing action of the Coulomb potential,[7] but the two approximations tend to converge at higher energies (indeed, they both become exact in the limit of infinite energy). However, it has proven difficult to establish a clear criterion for the energy range of validity of these approximations. Semiempirical approaches such as those of Lotz[10–12] and Drawin[13] have largely been used by those requiring ionization data. The proposed accuracy of

these approaches is modest (Lotz suggests accuracy of $^{+40}_{-30}\%$) but often sufficient. The semiempirical formula of Lotz[12] is

$$\sigma = \sum_{i=1}^{N} a_i q_i \frac{\ln(x)}{x E_i^2} \{1 - b_i \exp[-c_i(x-1)]\} . \tag{4}$$

Here x is the ratio of the energy of the impacting electron to E_i, with E_i the binding energy of electrons in the ith subshell, q_i the number of equivalent electrons in the ith subshell, and a_i, b_i, and c_i are "individual constants, which have to be determined by reasonable guesswork."[12] The form of this cross section is based upon the $x^{-1}\ln(x)$ behavior predicted by Bethe[14] for $x >> 1$, with the term in brackets included to modify the shape of the cross section near threshold. Unfortunately these semiempirical formulas occasionally fail badly, probably due to lack of explicit consideration of the indirect processes in Eqs. (1)–(3). It is essential therefore that the combination of experiment and legitimate theory be used to systematize the contributions from various mechanisms.

Zn^+ and Ga^+ are, respectively, Cu-like and Zn-like structures, with either one or two $4s$ electrons outside a closed $3d$ shell. While these particular ions are not normally found in CTR plasmas, heavier species stripped to these configurations may be present[15] in tokamaks in high enough abundances to be important in determining the energy balance via line radiation.

The only absolute experimental data for ionization of the $3d^{10}4s$ and $3d^{10}4s^2$ configurations are for Cu *I* and Zn *I*, respectively.[16–19] Presumably, due to difficulties in determining the target density and overlap factors with neutral targets, there are large discrepancies in the absolute values of the cross sections from various experiments. Additionally, there are cases where the shapes of the relative cross sections differ markedly among different investigations, implying large systematic relative errors (see, for example, comparison between Crawford[17] or Schroeer *et al.*[18] and Pavlov *et al.*[16] in Cu *I*).

Autoionizing configurations $3d^9 4s^2 4p$ and $3d^{10}4p^2$ have been attributed by Hashizume and Wasada[20] as the cause of structure in their observed relative ionization efficiency curve for Zn *I* in the threshold region. Similar structure has been observed in ionization efficiency curves for Cd and Hg.[21–23]

No experimental data exist for ionization of $3d^{10}4s$ and $3d^{10}4s^2$ configurations of ions, and the only calculations for these configurations are semiempirical,[12] or scaled-Born calculations for individual subshells.[6,8,9] The primary purpose of the present experiments is to elucidate the contribution of inner-shell ionization and excitation autoionization, and to provide data by which to judge the various calculational methods. In addition, a calculation of the excitation autoionization process is made for Zn^+.

II. EXPERIMENTAL PROCEDURE

A. Experimental technique and apparatus

The experiments consist of bombarding target ions with electrons of variable energy, and measuring the resulting production of doubly charged ions. The crossed-charged-beams technique was used, with beams of electrons and mass-analyzed ions intersecting at right angles in an ultrahigh vacuum environment. The primary and product ions are separated in a charge-state analyzer, the parent beam being directed to a Faraday cup and the doubly charged ions to an electron multiplier where they are individually counted. Figure 1 is a schematic view of the experimental arrangement.

With this experimental configuration, the ionization cross section is given in terms of experimental measurables by[24–28]

$$\sigma = \frac{\mathscr{R} e^2}{I_e I_i} \frac{v_i v_e}{(v_i^2 + v_e^2)^{1/2}} \frac{\mathscr{F}}{D_{++}} , \tag{5}$$

where I_i, I_i, v_e, v_i are the currents and velocities, respectively, of electrons and ions, D_{++} is the probability that a doubly charged ion produced by electron-impact will be detected, and $\mathscr{R}$ is the measured counting rate due to those ions. The former factor $\mathscr{F}$ takes account of the spatial overlap of the two beams, and is given by[25]

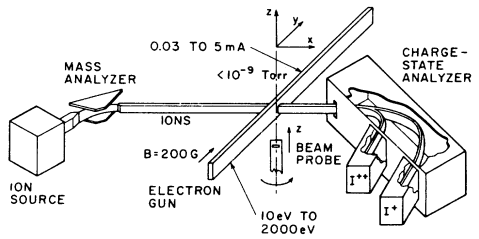

FIG. 1. Cross-charged-beams experimental arrangement.

$$\mathcal{F} = \frac{\int R(z)dz \int G(z)dz}{\int R(z)G(z)dz}, \quad (6)$$

where $R(z)$ and $G(z)$ are the relative vertical distributions of the electron- and ion-beam current densities.

The apparatus used for these experiments is similar to that used for previous experiments in this laboratory on electron-impact dissociation of positive molecular ions.[28] For the present experiments a magnetically confined electron gun[29,30] and improved beam probe[30,31] were used. Modifications to the analyzer include replacing the I^{++} Faraday cup with a large area electron multiplier for particle counting, and addition of a set of vertical deflection plates at the entrance slit to correct for the ion-beam deflection by the 200-G magnetic field of the magnetically confined electron gun. Full experimental details as well as results can be found in the thesis of Rogers.[27]

The ion source used for production of both Zn^+ and Ga^+ ions is a commercially available,[32] hot-cathode discharge ion source. For the Zn^+ experiment, pure Zn metal was introduced into the source via a stainless steel probe, while for Ga^+ ions a sample of GaI_3 was used. With both Zn^+ and Ga^+ ions, relatively stable beams of $\sim 0.2-0.3$ μA at 1 keV in the interaction region were obtained.

Zn^+ and Ga^+ both have metastable levels which may become populated in the ion source discharge. In the case of Zn^+ it was determined in auxiliary experiments that the effective lifetime[33] of metastable states is sufficiently short that essentially all these states decay during the ~ 50-μsec flight from the ion source to the interaction region. Furthermore, the source could be operated to minimize excited-state production such that the residual population of these states in the interaction region was $\lesssim 0.05\%$. In Ga^+, however, there are metastable levels whose lifetimes are sufficiently long (of order 0.5 sec or longer) that essentially all ions leaving the source in these states are still excited when they reach the interaction region. Thus the problem to be overcome with the Ga^+ ion source is to avoid production of metastables, or at least to measure their fraction and insure that it is small, so that determination of the ground-state target density may be known with high accuracy. Measurement of the metastable fraction was accomplished by measuring the ionization signal between the thresholds for metastable ionization and ground-state ionization, and using a theoretical[8,9] cross section to infer the target density of metastable ions. In this way it was possible to ascertain that during all of the relative cross section measurements the metastable population was less than 3%.[34]

B. Absolute calibration

The procedure used in the measurements reported here was to measure the relative cross section as a function of energy in great detail, to measure the absolute cross section using different procedures at only a few energies, then to normalize the relative curve to the absolute measurements. We measured the absolute cross section by using a calibrated vibrating reed electrometer to measure the total I^{++} current passing through the I^{++} slit at two different electron energies. We verified by a variety of tests[26] that the transmission of the analyzer for both the I^+ and I^{++} exit apertures is $100^{+0}_{-1.5}\%$, and that the collection efficiency of each ion collector is $100^{+0}_{-0.2}\%$. The relative cross section was measured by replacing analog current measurement at the I^{++} aperture with pulse counting detection in order to improve the statistical precision of the data.

An appreciable fraction of metastables in the beam (a problem only for Ga^+) during the measurement of the absolute cross section introduces an additional uncertainty. Consequently, when measuring the absolute ionization cross section of Ga^+ care was taken to keep the metastable content of the beam low, and the maximum metastable fraction during these measurements is estimated to have been 12%. Calculations of the $4s$ and $4p$ subshell ionization cross sections in the scaled PWB approximation[8,9] indicate that a metastable fraction of 12% leads to an uncertainty of less than 3% in the determination of the ground-state ionization cross section for Ga^+.

The measurements of the absolute cross sections were performed with dc beams. It was initially found that the electron beam produced no I^{++} current with the beam off; that is to say that there was no "electron background." This point was verified at electron energies from 20 eV to 2 keV. The measurements were repeated many times at each electron energy so that a statistical uncertainty could be assigned to the measurement of the mean of the samples. The results of the absolute ionization cross-section measurements for Zn^+ and Ga^+ appear in Table I with statistical and sys-

TABLE I. Zn^+, Ga^+ absolute ionization cross sections measured with the vibrating reed electrometer. Note that uncertainties are quoted at the 95% confidence level (see text).

Energy (eV)	$\sigma_{abs}(10^{-18}$ cm$^2)$ Zn^+	Ga^+
87.2	75.1±7.7%	
189	72.5±4.8%	78.3±4.8%
374	51.9±5.2%	56.0±5.4%

tematic errors, estimated at a level equivalent to the 95% confidence level (see Sec. II D).

C. Data accumulation and reduction

Following the measurements of the absolute cross section, summarized in Table I, the electron multiplier was used to measure the relative cross section as a function of energy. Form factors were measured regularly, and "benchmark" energies were returned to at regular intervals in any given data run to avoid problems associated with conceivable drifts (sensitivity, etc.) with time or other experimental conditions.

Table II indicates approximate ranges of beam currents and counting rates encountered in these experiments. The lower signal rates in the Ga^+ experiment compared to the Zn^+ experiment are due to reduced multiplier quantum efficiency, while the much lower background rates are primarily due to improved pressure in the interaction region.

D. Uncertainties

The crossed-charged-beams arrangement lends itself to various experimental diagnostics and systematic checks. As well as verifying that the cross section has the correct functional dependence on the quantities in Eqs. (5) and (6), it was demonstrated that the cross section was independent of background gas pressure, chopping frequency and scaler delays, and biases in the electron gun and collector. The remaining sources of statistical and systematic uncertainty are summarized in Table III. Statistical uncertainties have been evaluated at the 95% confidence level (95% CL) corresponding to two standard deviations. While we acknowledge that the term "confidence level" cannot be strictly applied to systematic uncertainties of a nonstatistical nature, an effort has been made to assess these uncertainties at a level consistent with the statistical 95% CL. The resulting net uncertainties are obtained by quadrature combination of the individual uncertainties, which are judged to be independent of one another.

TABLE II. Beam currents and counting rates.

	Zn^+	Ga^+
Electron-beam current	0.05–4	0.05–4 mA
Ion-beam current	0.1–0.3	0.06–0.3 μA
Background counting rate	3200–4000	450–1400 c s^{-1}
Signal counting rate	0–50000	0–30000 c s^{-1}

III. THEORETICAL CALCULATIONS

A significant contribution to ionization will be seen to come from an excitation-autoionization process [Eq. (3)]. In such a process, an inner-shell electron is excited and subsequently loses its energy by the ejection of a more loosely bound electron from an outer shell. We assume that all of the excited states will autoionize and we obtain the total ionization cross section by adding the sum of inner-shell excitation cross sections to the direct knock-on ionization cross section.

We use a two-state close-coupling approximation to calculate inner-shell excitation of Zn^+ for transitions $3d^{10}4s \rightarrow 3d^9 4snl$. The excited states considered are $^2P^o$, $^4P^o$, $^2F^o$, $^2D^o$, ^2P, and ^2D.

The orbitals used were described by Msezane and Henry[35] in a calculation of collision strengths for excitation of ground state Zn^+. With the CIV3 program of Hibbert,[36] we construct configuration-interaction wave functions to describe the target states. Excitation energies and configuration weights are given in Table IV. The dominant eigenstates are represented as follows:

$$^2P^o, ^2D^o, ^2F^o: \; c_1 3d^9 4s(^1D)5p + c_2 3d^9 4s(^3D)5p \; ,$$

$$^2D: \; c_1 3d^9 4s(^1D)5s + c_2 3d^9 4s(^3D)5s \; ,$$

$$^2P: \; c_1 3d^9 4s(^1D)5d + c_2 3d^9 4s(^3D)5d \; .$$

The coupled integro-differential equations are solved using the noniterative integral equation method of Smith and Henry.[37] Step sizes at small radial distances are chosen to be $0.0017a_0$. Ex-

TABLE III. Experimental uncertainties (95% CL).

	Zn^+	Ga^+
Absolute calibration uncertainties		
	6.8	
Statistical	3.2[a]	1.3[a]
	3.2	2.0
Vibrating reed electrometer calibration	1.5	1.5
Leakage resistance	1.0	1.0
Transmission of analyzer	1.5	1.5
I^{++} collection efficiency	0.2	0.2
Form factor	2.0	2.0
Electron path length	1.0	1.0
	0	
Uncollected electron current	0[a]	0[a]
	2.0	2.0
Electron-beam-current measurement	1.0	1.0
Ion-beam-current measurement	1.0	1.0
Metastable beam content	0	3.0
	7.7	
Quadrature sums	4.8[a]	4.8[a]
	5.2	5.4
Relative uncertainties		
Counting statistics	0.2% (typical)	
Form-factor fluctuations	0.3	
Detection efficiency fluctuations	0.2	
Ion-beam-current measurement	0.2	
Electron-beam-current measurement	0.2	
Quadrature sum	0.5%	

[a]Three values listed correspond consecutively to energies of 100, 200, and 400 eV.

TABLE IV. Energy differences and weight coefficients for eigenstates.

State	Eigenstate	c_1	c_2	ΔE (Ry)
1	$3d^{10}4s\,^2S$	1.0	0.0	0.0
2	$3d^9 4s(^3D)5p(^4P^o)$	0.0	1.0	1.356
3	$3d^9 4s(^1D)5p(^2F^o)$	0.798 77	0.601 64	1.393
4	$3d^9 4s(^1D)5p(^2P^o)$	0.829 35	0.558 73	1.398
5	$3d^9 4s(^1D)5p(^2D^o)$	0.791 48	0.611 20	1.404
6	$3d^9 4s(^3D)5p(^2P^o)$	0.558 73	−0.829 35	1.432
7	$3d^9 4s(^1D)5s(^2D)$	0.768 89	0.639 39	1.733
8	$3d^9 4s(^1D)5d(^2P)$	0.763 82	0.645 43	1.784

change terms are neglected at $r = 19.9a_0$, where the longest-ranged orbital has fallen to less than 10^{-3}.

IV. RESULTS

A. Data presentation

Cross sections for electron-impact ionization are presented in Figs. 2 and 3 for Zn^+ and Figs. 4 and 5 for Ga^+. The absolute points measured without the electron multiplier are shown with absolute total error bars in Figs. 2 and 4. Relative error bars on the bulk of the data points are too small to show, but as indicated in Table III are typically of order 0.5% (95% CL).

More than 900 data points were taken during the course of each experiment, with each data point being the average of from two to eight individual integrations at a given energy. The data in Figs. 2–5 represent interval averages of the raw data. In Figs. 3 and 5 the intervals are evenly spaced at 0.2 eV, with typically five measurements averaged together in each plotted point. The points in Figs. 2 and 4 are logarithmically spaced, and each is the average of typically six individual measurements. The points from 600 eV to 2 keV were taken with dc beams due to limitations on the electronics of our present scheme of chopping the electron beam at high voltages. However, the ion background was carefully subtracted by measuring the signal with and without the electron beam (the ion background at these energies was $\sim 10\%$ of the total count rate), and the electron background was verified to be zero for all electron energies.

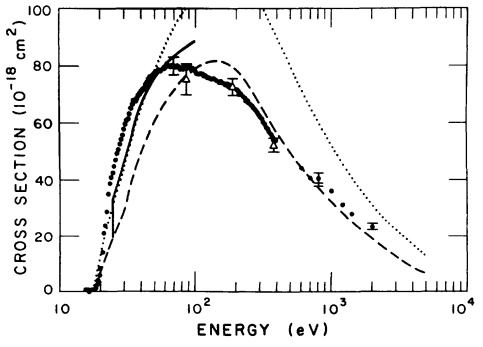

FIG. 2. Zn^+ ionization cross section—semilog plot. Solid points, present results; – – –, scaled PWB, McGuire (Refs. 8 and 9); ——, scaled PWB plus excitation autoionization; · · ·, semiempirical formula of Lotz (Ref. 11); ⧗, calibration points (see text). Error bars represent total absolute uncertainty at a level consistent with statistical 95% CL. Relative errors are for most points of the order of 0.5%, too small to show.

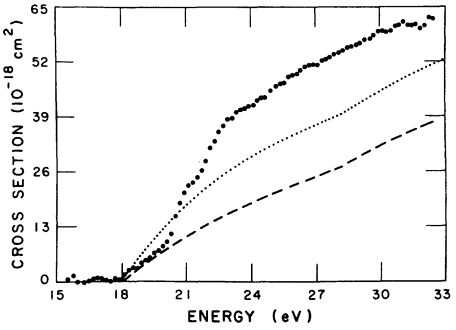

FIG. 3. Zn^+ ionization cross section in the threshold region. Symbols are the same as in Fig. 2.

B. Zn^+ ionization

In Fig. 2 the Zn^+ cross section is plotted against the logarithm of the incident energy. We see that the cross section rises to a peak value of 80.3 $\pm 2.4 \times 10^{-18}$ cm^2 at an energy of roughly 70 eV (3.9 times the threshold energy), above which it drops slowly until about 270 eV, at which energy it tends downward more rapidly. Referring to Fig. 3, the cross section rises approximately linearly for about the first 2 eV above threshold. Extrapolation of this linear region to the energy axis indicates that the threshold is located within 0.1 eV of the 17.96-eV ionization limit of Zn^+ determined spectroscopically.[38] At 20.5 eV the cross-section slope suddenly increases, and again at 22.0 eV. At about approximately 23 eV the slope resumes its initial value. The variation of points below the ionization threshold is not thought to be significant.

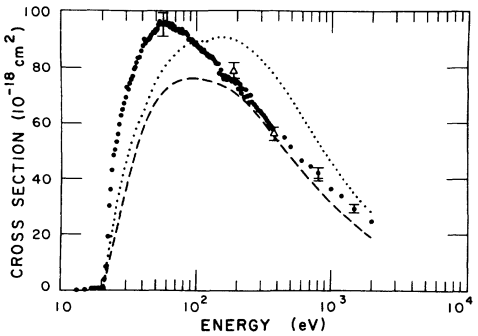

FIG. 4. Ga^+ ionization cross section—semilog plot. Symbols are the same as in Fig. 2.

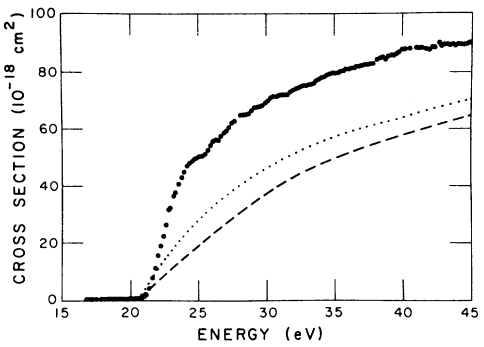

FIG. 5. Ga^+ ionization cross section in the threshold region. Symbols are the same as in Fig. 2.

The figures include plots of the total ionization cross section calculated using the Lotz semiempirical formula[12] and using the scaled PWB results of McGuire.[8,9] In all of the figures the dotted line is the Lotz prediction, and the dashed line is McGuire's. Ionization of the valence 4*s* electron plus the 3*d*, 3*p*, and 3*s* subshells were included in both approximations, using ionization potentials in Table V for individual subshells. In addition, in Fig. 2 the solid line gives the sum of our inner-shell excitation cross sections and the scaled PWB results for direct ionization.

Figure 3 indicates that the agreement between experiment and scaled PWB for the first 2 eV above threshold is excellent. Above this energy the experimental curve exceeds the scaled PWB, and remains larger to above 100 eV. There are at least two explanations for this discrepancy. First, the PWB approximation ignores the focusing action of the Coulomb potential of an ion upon the incident electron. Peach[17] has shown in comparisons between PWB and Coulomb-Born (CB) ionization calculations that the PWB results are consistently lower than the CB results from threshold to somewhat above the peak of the cross-section curve, and furthermore, that use of the PWB approximation for ions shifts the cross-section peak toward higher energies.

TABLE V. Subshell ionization energies (in eV) for Zn^+ and Ga^+. Numbers in parentheses are references.

Subshell	Zn^+	Reference	Ga^+	Reference
4*s*	17.96	(38)	20.51	(38)
3*d*	27.8	(38)	39.6	(39)
3*p*	113	(40)	118	(40)
3*s*	135.9	(41)	158.1	(41)

Second, we have found that excitation autoionization plays an important role in the near-threshold ionization cross section of Zn^+. Figure 6 shows the derivative of the experimental data from Fig. 3. The derivative has been treated with a single three-points smoothing, and the uncertainties (shown in the figure by a single flag above the curve) are deduced from the reproducibility of the derivative spectra from five individual data runs. A peak in such a derivative spectrum would be expected for an excitation-autoionization process, which may be roughly characterized as having a step threshold typical of electron-ion excitation, if one ignores the broadening of the upper state produced by configuration interaction with the continuum.[15] The peak width is expected to be characteristic of the energy spread of the electron beam. In Fig. 6, the first prominent peak, centered at 20.5 eV, has a width consistent with the energy spread of the electron beam. The second peak, at 22.0 eV, is slightly broader, and has a shoulder on the high-energy side which was consistently reproducible. Hence, we might conclude that the first peak is due to excitation autoionization through a single resonant state, and the second peak contains the contribution from two or more resonant states, or is broadened by configuration interaction. It will be noted from the size of the error bar in the figure that one cannot make definitive statements about the apparent structure beyond 24 eV.

We note in Fig. 6 that the continuum background due to direct knock-on ionization has the same slope immediately before and after the two large peaks. Thus it is reasonable to assume that the direct process may be approximated by a linear function, and making this approximation, we find from Fig. 3 that the contribution to the total cross

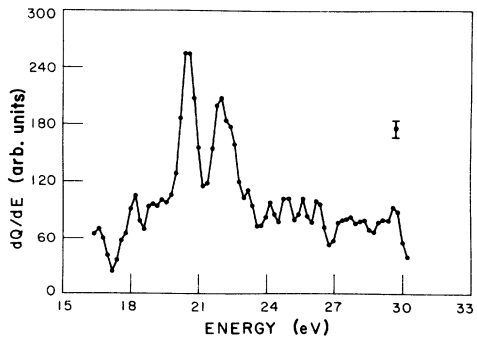

FIG. 6. Derivative with respect to energy of the ionization cross section for Zn^+. Error bars above the curves represent rms reproducibility of derivatives from individual data runs.

section from excitation autoionization leads to an enhancement by a factor 2.4 at 23 eV, and a factor of 2.0 at 30 eV.

The PWB approximation of McGuire is a simple independent-particle model, and inherently lacks the ability to account for excitation-autoionization processes. Thus, we calculate cross sections for excitation of an inner-shell $3d$ electron and add them to the direct knock-on ionization results of McGuire. Inner-shell excitation cross sections are given in Table VI for energies from near threshold to approximately five times threshold for excited states $^2P^o$ and $^4P^o$. The summed excitation to all other states is estimated to be at least a factor of 2 less than that of $3d^9 4s(^1D)5p\ ^2P^o$. This estimate is based on a comparison of the two major partial-wave contributions for all the states.

We obtain an excitation-autoionization contribution to the total ionization cross section of 16×10^{-18} cm^2 from the states dominated by $3d^9 4s(^1D)5p\ ^2P^o$. In addition, we estimate a summed contribution of 9×10^{-18} cm^2 from a number of states $3d^9 4s\,5l$ clustered at higher energies. The threshold energies of the states are not in good agreement with experiment since the orbitals were optimized to yield a good description of the low-lying states of Zn^+. Thus, the first major threshold is calculated to be at 19.0 eV due to the $3d^9 4s\,4p$ state, whereas the experimental data indicate a threshold at 20.5 eV.

In Fig. 2, the solid curve gives the sum of the direct plus excitation-autoionization contributions to the total ionization cross section. Experiment and theory are in good agreement for impact energies up to 60 eV. At higher energies, differences between theory and experiment are probably due to the inaccuracy of the PWB approximation for direct ionization.

The contribution of autoionization to the total ionization cross section was calculated by Cowan and Mann[42] for sodiumlike ions. They also predict in the same reference that excitation autoionization in the Cu and Zn isoelectronic sequences should be important, and that prediction is here verified (also see the Ga^+ results below).

The role of excitation autoionization has been verified experimentally for the singly charged alkali like ions Mg^+, Ca^+, Sr^+, and Ba^+ (see the review by Dolder and Peart, Ref. 24 and references therein). A fivefold increase due to the onset of excitation autoionization in the ionization cross section of Ba^+ was found, with smaller but still significant contributions in Sr^+ and Ca^+. Only in Mg^+ was there no observed enhancement. The interpretation was that *np-nd* transitions were largely responsible for the autoionization, whereas no such transition exists in Mg^+ ($2d$ states do not exist). Recent work on Li-like ions[43–45] Be^+, C^{3+}, N^{4+}, O^{5+}, and on Na-like ions[46] Al^{2+} and Si^{3+} also show clear excitation-autoionization contributions. Recently, factors of 10–30 enhancement of the ionization cross section due to excitation autoionization have been observed.[47]

Referring to Fig. 2, we see that the experimental cross section peaks at an energy lower than either the Lotz curve or the scaled PWB result. We expect that this is due to enhancement of the low-energy cross section by excitation autoionization and to the focusing action of the Coulomb potential (the constants in the Lotz formula were determined mostly by fitting to neutral-atom ionization cross sections and so presumably will tend to ignore the Coulomb nature of the potential in electron-ion collisions). Also, at energies near the peak of the scaled PWB result the experimental curve is relatively flat, but at higher energies more closely resembles the shape of the scaled PWB curve. This shape is probably due to the increasing fractional contribution from $3d$ subshell ionization as the excitation autoionization and outer-shell contributions begin to die off.

We note in passing that the scaled PWB calculation produces a peak cross section agreeing within 2.5% with the experimental peak cross section, al-

TABLE VI. Cross section (10^{-18} cm^2) vs electron energy E (eV).

Transition[a]/E	25	30	40	60	100
1–4	16.2	16.3	15.8	13.8	9.9
1–6	3.4	3.6	3.6	3.1	2.2
1–2	0.94	0.61	0.33	0.13	0.04

[a]See Table IV.

though it is shifted in energy. This remarkable agreement would presumably worsen with use of the more "correct" CB approximation, which usually produces a larger peak cross section. Since McGuire's scaling is obtained from the peak value of the cross section, care should be exercised in extending such scaling along isoelectronic sequences. Indeed, McGuire[8,9] has found that for isoelectronic sequences with outer shells of low ionization potential, the scaling obtained by the PWB approximation for neutral atoms is not valid.

Not included in the figures are the classical binary-encounter results by Gryzinski[48] and Mathur *et al.*[49] These results greatly overestimate the peak cross section, Gryzinski by a factor of 3 and Mathur *et al.* by a factor of ~ 5. Also not included are results using the scaled infinite Z CB method of Sampson and Golden.[6] That this method is inaccurate for ions of low charge as stated by the authors is indicated by the factor of ~ 3 discrepancy with our experiments at 2 keV.

C. Ga^+ ionization

The comments in Sec. IV A regarding the accumulation and reduction of the ionization data and error estimates apply in the case of the Ga^+ ionization data. A few additional comments should be made here.

First, as pointed out in Sec. II B the presence of metastables in the calibration of the absolute value of the Ga^+ ionization curve leads to a small additional uncertainty in the absolute calibration, included in the error bars in the data. Second, all of the relative data were taken with a beam metastable fraction of 3% or less, as determined by tests before and after each data run of the signal at approximately 18 eV. The unimportance of the small metastable contamination may be appreciated by observing the data below threshold in Figs. 4 and 5. Third, between the Zn^+ and Ga^+ ionization experiments a factor of 6 improvement in the final chamber pressure was realized, from 4×10^{-7} Pa (3×10^{-9} Torr) to 6.5×10^{-8} Pa (5×10^{-10} Torr). This resulted in superior signal-to-noise ratio and much better precision in the relative data, particularly near threshold.

Referring to Fig. 5 we see that below the threshold for ionization of ground-state Ga^+ ions at 20.51 eV there is a small nonzero cross section due to $<3\%$ contamination by $3d^{10}4s4p\ ^3P_{0,2}$ metastables. Routine checks below the 14.5-eV threshold for metastable ionization showed a zero cross section with high precision (the cross section below 14.5 eV was always $0\pm0.1\times10^{-18}$ cm^2, or $\sim10^{-3}$ of the Ga^+ peak ionization cross section).

Immediately above threshold the cross section rises rapidly, and examination of Fig. 5 reveals a series of small oscillations in the cross section from about 22 eV to about 35 eV. These oscillations will be discussed more completely below.

Figure 4 shows that the cross section reaches its peak value of $92.1\pm4.5\times10^{-18}$ cm^2 at approximately 55 eV, then falls smoothly. At high energy the cross section is following the generally predicted $E^{-1}\ln E$ dependence.

Figure 7 is a plot of the derivative of the data in Fig. 5. Uncertainties (indicated by the single flag above the curve) are deduced from the scatter of the derivative spectra calculated from the six individual data runs used to obtain the average shown in Fig. 5. As is now apparent, the oscillations in the data of Fig. 5 mentioned above are statistically significant, and in analogy to the discussion for Zn^+ are interpreted as arising from excitation autoionization. The peaks in Fig. 7 immediately above threshold appear to be three partially resolved peaks. The remaining features tend to grow smaller as they get farther from threshold. The improved statistics in this derivative spectrum over the Zn^+ derivative spectrum (Fig. 6) are due to the improved final chamber vacuum. Positions of about 50 autoionizing states of Ga^+ from threshold to 33 eV above the ground state of Ga^+ have been recently calculated,[50] with configurations $3d^{10}n\ln'l'$. Though some correlation with observed structures in Fig. 7 can be noted, it is not possible to make identifications due to the density of states and lack of transition probability data. It is likely that much of the excitation autoionization observed results from $3d^9 4s^2 nl$ levels. Pindzola *et al.*[51] have calculated cross sections and fine-structure splittings for the three $j=1$ levels of the

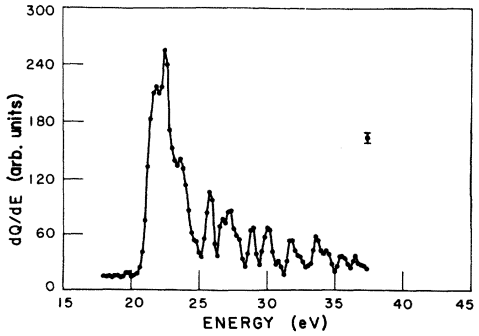

FIG. 7. Derivative as in Fig. 6, except data are for Ga^+.

configuration $3d^9 4s^2 4p$, as well as branching ratios to the continuum. They find reasonable agreement with the splittings of the three partially resolved peaks near threshold in Fig. 7 as well as good agreement with the observed contributions to the cross section.

Again, as in the case of Zn^+ ionization, we show the calculation for ionization of Ga^+ in the scaled PWB approximation of McGuire.[8,9] We also inlcude the semiempirical results of Lotz[12] for comparison. Subshell ionization potentials used for both approximations are listed in Table V.

Figures 4 and 5 show the underestimate of both the scaled PWB and the Lotz formula from threshold up to the peak of the experimental cross section. Examination of the derivative spectrum (Fig. 7) gives an indication that the cross section from threshold to above 30 eV is dominated by excitation autoionization, although a quantitative estimate of the fractional contribution is more difficult than in the case of Zn^+ due to lack of a quasilinear region at threshold. Nevertheless, if we make the rough assumption that the scaled PWB results give an indication of direct ionization in this region, we arrive at enhancement factors of 2.5 at 25 eV and 1.6 at 35 eV, comparable to the enhancement of the Zn^+ ionization cross section. The enhancement factors arrived at above are presumably somewhat overestimated because we have ignored the fact that use of the Coulomb-Born approximation should lead to a larger prediction of the direct cross section near threshold. However, agreement with our theoretical estimates and those of Pindzola *et al.*[51] along with the marked structure indicated in Figs. 6 and 7 lead us to believe that enhancement due to excitation autoionization is important. This is in accord with the prediction of Cowan and Mann[42] of the importance of autoionization in the total ionization cross section for the Zn isoelectronic sequence.

In the region of the cross-section peak the situation in Ga^+ is somewhat different than in Zn^+. The scaled PWB results for Ga^+ underestimate the cross section considerably, while the Lotz formula gives reasonable agreement with the peak value of the cross section, though both approximations produce a peak shifted toward higher energy from the experimental curve. Use of the CB rather than PWB approximation should improve agreement, though we expect that inclusion of excitation autoionization will still be important in obtaining accurate near-threshold results.

Looking more closely at the Lotz formula predictions for Zn^+ and Ga^+ we notice that excellent agreement is obtained above about 150 eV for both ions if the Lotz "a_i" coefficient for the $3d$ subshell is reduced by about a factor of 2, from 2.9×10^{-14} to 1.5×10^{-14} cm^2 eV^2 (this sort of adjustment is reasonable in light of the fact that at the time Lotz deduced the parameters for $3d$ electrons no experimental data existed for ionization from this subshell). With this adjustment the Lotz formula is also brought into good agreement with the scaled PWB approximation. It is now apparent that the greater enhancement from threshold to peak of the experimental curves over both calculations (scaled PWB and revised Lotz) for Ga^+ as compared with Zn^+ is probably due to significantly larger contributions from excitation autoionization in the former.

As in the case of Zn^+, results using the classical method of Gryzinski[48] were not plotted, since the curve is well off the scale of the figure, overestimating the experimental results by a factor of $\sim$2.5. Again, as in the case of Zn^+, the prediction using the method of Sampson and Golden[6] seriously underestimates the cross section at 2 keV.

IV. CONCLUSION

Absolute cross sections for single ionization of Zn^+ and Ga^+ by electron impact have been measured from below threshold to 2 keV. The role of excitation autoionization was clearly demonstrated to be of major importance at impact energies within a factor of 2 of the threshold energy, enhancing the ionization cross section by up to a factor of about 2.5. It is emphasized that without data of high precision and resolution, these effects would have been obscured.

Comparison with the scaled PWB calculations of McGuire shows satisfactory agreement at high energy, with substantial disagreement in the threshold region, presumably due in part to omission of excitation-autoionization channels. Most of this disagreement is removed for Zn^+ when inner-shell excitation cross sections are added to the scaled PWB results. Similar calculations for Ga^+ were made by others.[51] Comparison with the widely used Lotz formula shows disagreement well beyond the uncertainties estimated by Lotz, but dividing the coefficient for $3d$ subshell ionization by 2 yields results which are in agreement with experiment to within Lotz's $^{+40}_{-30}$% uncertainty, except in the threshold region, again due to omission of excitation autoionization.

ACKNOWLEDGMENTS

We are grateful to G. Victor and to M. Pindzola for communicating their results prior to publication. Thanks are also due to W. C. Lineberger, and D. W. Norcross for several helpful discussions. This work was supported in part by the Office of Magnetic Fusion Energy, U.S. Department of Energy, and the Office of Basic Energy Sciences, U.S. Department of Energy.

---

*Present address: Radiation Physics Division, National Bureau of Standards, Gaithersburg, Maryland 20234.
†Permanent address: Laboratorio Metod Av Inorganiche, CNR, Rome, Italy.
‡Staff Member, Quantum Physics Division, National Bureau of Standards, Gaithersburg, Maryland 20234.
§Present address: Physics Department, Morehouse College, Atlanta, Georgia 30314.

[1]D. L. Moores, J. Phys. B 5, 286 (1972).
[2]D. L. Moores, J. Phys. B 11, L403 (1978).
[3]D. L. Moores and H. Nussbaumer, J. Phys. B 3, 168 (1970).
[4]E. Stingl, J. Phys. B 5, 1160 (1972).
[5]S. M. Younger, Phys. Rev. A 22, 111 (1980); 22, 1425 (1980); 23, 1138 (1981); 24, 1272 (1981); 24, 1278 (1981).
[6]D. H. Sampson and L. B. Golden, J. Phys. B 11, 541 (1978).
[7]G. Peach, J. Phys. B 4, 1670 (1971).
[8]E. J. McGuire, Phys. Rev. A 16, 62 (1977).
[9]E. J. McGuire, Phys. Rev. A 16, 73 (1977).
[10]W. Lotz, Astrophys. J. Suppl. 14, 207 (1967).
[11]W. Lotz, Z. Phys. 216, 241 (1968).
[12]W. Lotz, Z. Phys. 220, 466 (1969).
[13]H. W. Drawin, Z. Phys. 164, 513 (1961); correction in Z. Phys. 168, 288 (1962).
[14]H. Bethe, Ann. Phys. 5, 325 (1930).
[15]M. J. Seaton, in *Advances in Atomic and Molecular Physics,* edited by D. R. Bates and B. Bederson (Academic, New York, 1975), Vol. 4, p. 83.
[16]S. I. Pavlov, V. I. Rokhovskii, and G. M. Fedorova, Zh. Eksp. Teor. Fiz. 52, 21 (1967) [Sov. Phys.—JETP 25, 12 (1967)].
[17]C. K. Crawford, Air Force Technical Report No. AFML-TR-67-376, 1967 (unpublished).
[18]J. M. Schroeer, D. H. Gündüs, and S. Livingston, J. Chem. Phys. 56, 5135 (1973).
[19]R. F. Pottie, J. Chem. Phys. 44, 916 (1966).
[20]See, for example, A. Hashizume and N. Wasada, Jpn. J. Appl. Phys. 18, 429 (1979) and references therein.
[21]W. M. Hickam, Phys. Rev. 95, 703 (1954).
[22]B. Cabaud, A. Hoareau, P. Nounou, and R. Uzan, Int. J. Mass Spectrom. Ion Phys. 8, 181 (1972).
[23]C. E. Kuyatt, J. A. Simpson, and S. R. Mielczarek, Phys. Rev. 138, 385 (1965).
[24]K. T. Dolder and B. Peart, Rep. Prog. Phys. 39, 693 (1976).
[25]M. F. A. Harrison, in *Method in Experimental Physics,* edited by W. L. Fite and B. Bederson (Academic, New York, 1968), Vol. 7A, pp. 95–115.
[26]G. H. Dunn, in *Atomic Physics,* edited by V. W. Hughes, B. Bederson, W. W. Cohen, and F. M. J. Pichanick (Plenum, New York, 1969), pp. 417–433.
[27]W. T. Rogers, Ph.D. thesis, University of Colorado, 1980 (unpublished) (available through University Microfilms, Ann Arbor, Michigan).
[28]G. H. Dunn and B. Van Zyl, Phys. Rev. 154, 40 (1967).
[29]P. O. Taylor, K. T. Dolder, W. E. Kauppila, and G. H. Dunn, Rev. Sci. Instrum. 45, 538 (1974).
[30]P. O. Taylor, Ph.D. thesis, University of Colorado, 1972 (unpublished) (available through University Microfilms, Ann Arbor, Michigan).
[31]P. O. Taylor and G. H. Dunn, Phys. Rev. A 8, 2304 (1973).
[32]M. Menzinger and L. Wahlin, Rev. Sci. Instrum. 40, 102 (1969).
[33]The Zn^+ ($3d^9 4s^2\,^2D_{3/2}$) lifetime has been previously measured [L. D. Schearer and W. C. Holton, Phys. Rev. Lett. 24, 1214 (1970); A. L. Osherovich, Ya. F. Verolainen, and V. I. Privalov, Opt. Spectrosc. (USSR) 46, 617 (1979)] to be of order 2 μsec. We have measured an effective lifetime of radiation from this state to be 15.3 μsec, and have determined that this value is affected by cascade from higher states such as $3d^9 4s(^1D)4p(^2P)$ or $3d^9 4s(^1D)4p(^2D)$. In any case, even with a lifetime of 15.3 μsec only 3.8% of the original metastable population remains at the interaction region.
[34]Note that the scaled PWB theory of McGuire underestimates the cross section near threshold for ionization of the $4p$ subshell due to exclusion of excitation autoionization and the use of plane waves where Coulomb waves are appropriate. Thus our assessments of metastable fraction are overestimates.
[35]A. Z. Msezane and R. J. W. Henry (unpublished).
[36]A. Hibbert, Comput. Phys. Commun. 9, 141 (1975).
[37]E. R. Smith and R. J. W. Henry, Phys. Rev. A 7, 1585 (1973).
[38]C. E. Moore, *Atomic Energy Levels,* Natl. Bur. Stds. (U.S.) Circ. No. 467 (U.S. GPO, Washington, D.C., 1958).
[39]Y. N. Joshi, K. S. Bhatia, and W. E. Jones, Spectrochim. Acta, Part B 28, 149 (1973).
[40]E. Clementi and C. Roetti, At. Data Nucl. Data Tables 14, 177 (1974).
[41]J. A. Bearden, Rev. Mod. Phys. 39, 1 (1967); and assuming that $3s$ binding energy is the same in A^+ as in

A, where *A* =Zn or Ga.
[42]R. D. Cowan and J. B. Mann, Astrophys. J. 232, 940 (1979).
[43]R. A. Falk and G. H. Dunn (private communication).
[44]D. H. Crandall, R. A. Phaneuf, and P. O. Taylor, Phys. Rev. A 18, 1911 (1978).
[45]D. H. Crandall, R. A. Phaneuf, B. E. Hasselquist, and D. C. Gregory, J. Phys. B 12, L249 (1979).
[46]D. H. Crandall, R. A. Phaneuf, R. A. Falk, D. S. Belić, and G. H. Dunn, Phys. Rev. A 25, 143 (1982).
[47]R. A. Falk, G. H. Dunn, D. C. Griffin, C. Bottcher, D. C. Gregory, D. H. Crandall, and M. S. Pindzola, Phys. Rev. Lett. 47, 494 (1981).
[48]M. Gryzinski, Phys. Rev. 138, A336 (1965).
[49]K. C. Mathur, A. N. Tripathi, and S. K. Joshi, Int. J. Mass Spectrom. Ion Phys. 4, 483 (1970).
[50]G. A. Victor and W. R. Taylor, At. Data Nucl. Data Tables (in press).
[51]M. S. Pindzola, D. C. Griffin, and C. Bottcher, Phys. Rev. A 25, 211 (1982); see also Bull. Am. Phys. Soc. 26, 823 (1981).